

Multi-material distributed recycling via Material Extrusion: rHDPE and rPET case of study

Catalina Suescun Gonzalez^{1,2,3}, Fabio A. Cruz Sanchez¹, Hakim Boudaoud¹, Cécile Nouvel²,
Joshua Pearce³

¹Université de Lorraine – ERPI – F-54000, Nancy, France

²Université de Lorraine, CNRS, LRGP, F-54000 Nancy, France

³Western University, Department of Electrical & Computer Engineering, Canada, London

Abstract

The high volume of plastic waste and the extremely low recycling rate have created a serious challenge worldwide. Local distributed recycling coupled with additive manufacturing (DRAM) offers a solution by economically incentivizing local recycling. One DRAM technology capable of processing large quantities of plastic waste is fused granular fabrication (FGF), where solid shredded plastic waste can be reused directly as 3D printing feedstock. This study presents an experimental assessment of multi-material recycling printability using two of the most common thermoplastics in the beverage industry, polyethylene terephthalate (PET) and high-density polyethylene (HDPE), and the feasibility of mixing PET and HDPE to be used as a feedstock material for large-scale 3-D printing. After the material collection, shredding, and cleaning, the characterization and optimization of parameters for 3D printing were performed. Results showed the feasibility of printing a large object from rPET/rHDPE flakes, reducing the production cost by up to 88%.

Acronyms

Acronym	Definition
ABS	Acrylonitrile Butadiene Styrene
AM	Additive Manufacturing
DRAM	Distributed recycling via additive manufacturing
DSC	Differential scanning calorimetry
FDM	Fused deposition modeling
FFF	Fused filament fabrication
FGF	Fused granular fabrication
FPF	Fused particle fabrication
FTIR	Fourier-transform infrared spectroscopy
HDPE	High-density polyethylene
MFI	Melt flow index
PC	Polycarbonate
PET	Poly(ethylene terephthalate)
PLA	Poly(lactic acid)
PP	Polypropylene
PSO	Particle swarm optimization
PS	Polystyrene
SEBS	Poly (styrene-block-ethene-co-butene-block-styrene)
Tg	Glass temperature
pBC	Printed Bottle-Cap
rHDPE	Recycled High-density Polyethylene
rPET90//rHDPE10	Recycled Bottle-Cap (Cristaline bottle shredded without separation)
rPET	Recycled Poly(ethylene) terephthalate
vPET	Virgin or commercial Poly(ethylene terephthalate)

Introduction

- 1 The disposal of plastic waste is one of the most challenging current environmental concerns given its systemic
2 complexity [1]. The mass of micro- / meso- plastics in the oceans is expected to exceed the mass of the
3 global stock of fish by 2050 [2]. More critically, the global annual plastic production is expected to reach 1100
4 metric tons by the same year [3]. Societal awareness of plastic recycling has received substantial attention from
5 scientists, policymakers, and the general public [4]. Unfortunately, the statistical analysis of the centralized
6 recycling process proves that it has been largely ineffective [5] with only 9% of the plastic produced since
7 1950 being recycled from the total stock [6]. Therefore, it remains an open challenge to identify alternatives
8 to valorize discarded plastic material.
- 9 Distributed recycling and additive manufacturing (DRAM) is an innovative technical approach to recycling
10 plastic waste [7], [8]. DRAM was initially implemented using recyclebots, which are waste plastic extruders
11 that produce filament for conventional fused filament-based 3-D printers [9]–[11]. Previous studies have
12 shown that distributed recycling aligns with the circular economy paradigm [12], [13]. This approach allows

13 consumers to directly recycle their own waste into consumer products using open-source designs, ranging from
14 toys for children [14] to adaptive aids for individuals with arthritis [15]. Distributed manufacturing is now
15 widely adopted [16]. In this way, DRAM-based recycling operates within a closed-loop supply chain network
16 [17]. The primary goal of this type of recycling is to reduce the environmental impact by minimizing the
17 transportation from the waste source to recycling facilities [18]. In that sense, it aims to propose innovative
18 closed-loop strategies that utilize waste materials as raw resources [19].

19 Fused filament fabrication (FFF, which is also known as Fused Deposition Modelling –FDM®-) is the most
20 widespread and established extrusion-based AM technology. It has gained popularity due to the open-source
21 proliferation from the self-replicating rapid prototyper (RepRap) project [20]–[22]. FFF is favored for its sim-
22 plicity, versatility, low cost, and ability to construct complex geometric objects in the industrial and prosumer
23 domains [19]. Indeed, the open-source approach for 3-D printing has facilitated significant advancements in
24 manufacturing and prototyping adding value to the recycled material [7]. Efforts are being made to identify
25 sustainable feedstocks for 3-D printing [24]. Several studies have expanded the range of recycled filament
26 materials including PLA [25], [26], ABS [27], [28], PET [29], [30], HDPE [9], [27], [31], and PC [32]. In fact,
27 [18] conducted a comparative life cycle assessment in a low-density population case study in Michigan (USA)
28 and estimated that a distributed approach could save approximately 100 billion MJ of energy per year from
29 the recycling of 984 million pounds of HDPE. There is substantial evidence that DRAM can contribute to
30 reducing energy consumption and greenhouse emissions in manufacturing processes.

31 Most DRAM studies have used mono-materials for the fabrication of feedstock for FFF. There are, however,
32 several examples of mixed materials including wood waste and recycled plastic [33], [34] and textile fibers
33 and recycled plastic [35]. Recently, [36] reported the manufacturing of composite filament from recycled
34 PET/PP and PS/PP blending through a compatibilizer copolymer such as SEBS. Their results revealed the
35 technical printability of polypropylene blend composite filaments from a thermo-mechanical characterization
36 perspective. Increasing the performance window of blending materials by compatibilization which could be
37 a relevant path for recycling plastics at a local level and in isolated areas contexts (e.g. during humanitarian
38 crises [37]–[39], supply chain disruptions [40], [41], [42], [43] and/or isolated off-grid situations using solar-
39 powered 3-D printers [44]–[47]). Likewise, [30] studied the evaluation of the microstructure, mechanical
40 performance, and printing quality of filaments made from rPET and rHDPE varying the wt% of HDPE
41 material from 0 to 10%. They confirmed the increase in Young's modulus from 1.7 GPa of the pure PET to
42 2.1 GPa for all the HDPE concentrations. Additionally, the maximum stress of the bends was augmented
43 with high HDPE concentrations. Values were lower than virgin PET filament, yet similar to commercial
44 recycle ones. The addition of rHDPE at higher levels, however, helped to meet the brittle-ductile transition
45 in 15% despite the low interfacial tension of both polymers, allowing the printing of quality parts.

46 While former studies have proven successful in FFF, a new approach to DRAM is fused granular fabrication
47 (FGF) or fused particle fabrication (FPF), where the material-extrusion AM systems print directly from
48 pellets, granules, flakes, shreds or grinder material [11], [48]. In the context of recycling, this could reduce
49 the number of melt/extrusion cycles that degrade the material needed in the filament fabrication process
50 [25]. The FGF technique opens up the potential to use recycled materials as well as print large-scale objects
51 either with a conventional cartesian 3-D printer [11], delta 3-D printer [49] or hangprinter [50], [51]. Research
52 groups have corroborated that plastic waste can be used as feedstock materials for FGF/FPF. [52] assessed
53 the technical and economical dimensions of virgin and shredded PLA printed in a self-modified FGF machine
54 and compared it with FFF. The investigation showed that the use of FGF reduced printing costs, time and
55 its mechanical performance was comparable to that obtained using the traditional FFF technique. Likewise,
56 [11] found comparable properties between PLA, ABS, PP, and PET recycled and virgin materials. Later
57 publications demonstrated the technical and economic feasibility through the printing of complex objects
58 validating the possibility of recycling plastic with FGF in both conventional and common FFF materials [53],
59 but also recycling PC [54] and rPET [55]. Few researchers, however, have addressed the problem of directly
60 printing recycled multi-materials, which might be a key step forward needed to facilitate the ease of sorting
61 and recycling post-consumer plastic waste materials.

62 This study explores the potential of direct 3-D printing of two immiscible polymers commonly used in the
63 beverage sector through a distributed recycling process for its easy implementation operation at the local
64 level. To demonstrate the feasibility of the process, the most commonly used plastic for bottled water in
65 France, which consists of roughly 90% PET (body of the bottle) and 10% HDPE (cap) now referred to as
66 *rPET90//rHDPE10*, is used as a test material. The experimental process of collection, characterization, and
67 printing of the recycled material is described, and the results are discussed in the context of widespread
68 DRAM adoption at the community-based level.

69 Materials and Methods

70 The methodology presented in Figure 1 outlines the approach adopted to develop the study. The three stages,
71 namely *Material obtention*, *Printing process*, and *Evaluation* were thoroughly studied to control the major
72 process steps and the technical characterization methods. In the following subsections, each step is explained.

73 Raw material obtention

74 The goal of the material stage is to collect and prepare post-consumer plastic sources. In this study, water
75 bottles coming from the French brand Cristaline[®] were used as feedstock. The process steps used are shown in

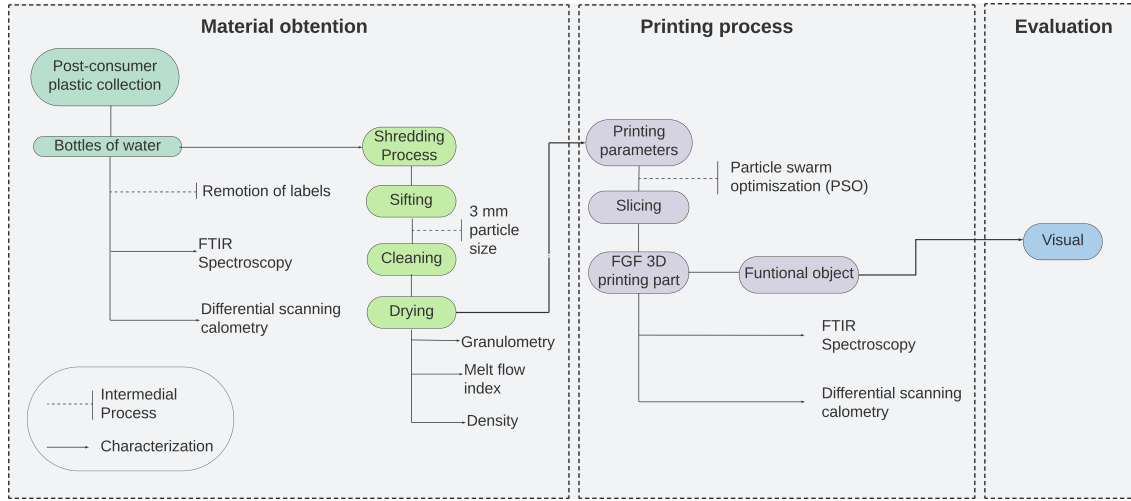


Figure 1: Global framework of the study

76 Figure 2 a/b. Post-consumer bottles were collected from receptacles placed in partnership schools in Lorraine,
 77 France. To convert the complete water bottles including their caps into 3DP feedstock material, the labels
 78 were removed before shredding in a cutting mill (Retsch MS300) using a 3 mm grid. After shredding, the
 79 obtained flakes were sifted with a 1.5 mm, 3 mm, and 5 mm sifters for further analysis. Next, the flakes were
 80 cleaned with hot water in an ultrasonic machine at 60°C for 1 hour to remove contaminants. Lastly, they
 81 were dried in a conventional oven overnight at 80°C [56], [57] to avoid degradation of the material. Washing
 82 conditions were the same for all the samples; therefore, the effect of contaminants was not considered. The
 83 resultant material is shown in Fig 2.c.

84 The material composition was calculated as a function of the mass of the bottles and caps separately. The
 85 percentage (%) of bottle-cap was found to be ~90% rPET (bottle) and ~10% rHDPE (cap). The complete
 86 bottle was shredded without separation of both materials thus this percentage is constant for all the samples.

87 Material preparation and characterization

88 Material particle size analysis -Granulometry-

89 In order to ensure the particle size suitable for printing, the granulate particles were characterized using the
 90 open-source ImageJ software [58]. The size characteristics of the particles were evaluated in four different
 91 samples: vPET (used as a reference) and the raw material sifted into three different sizes: 1.5 mm, 3 mm,
 92 and 5 mm.

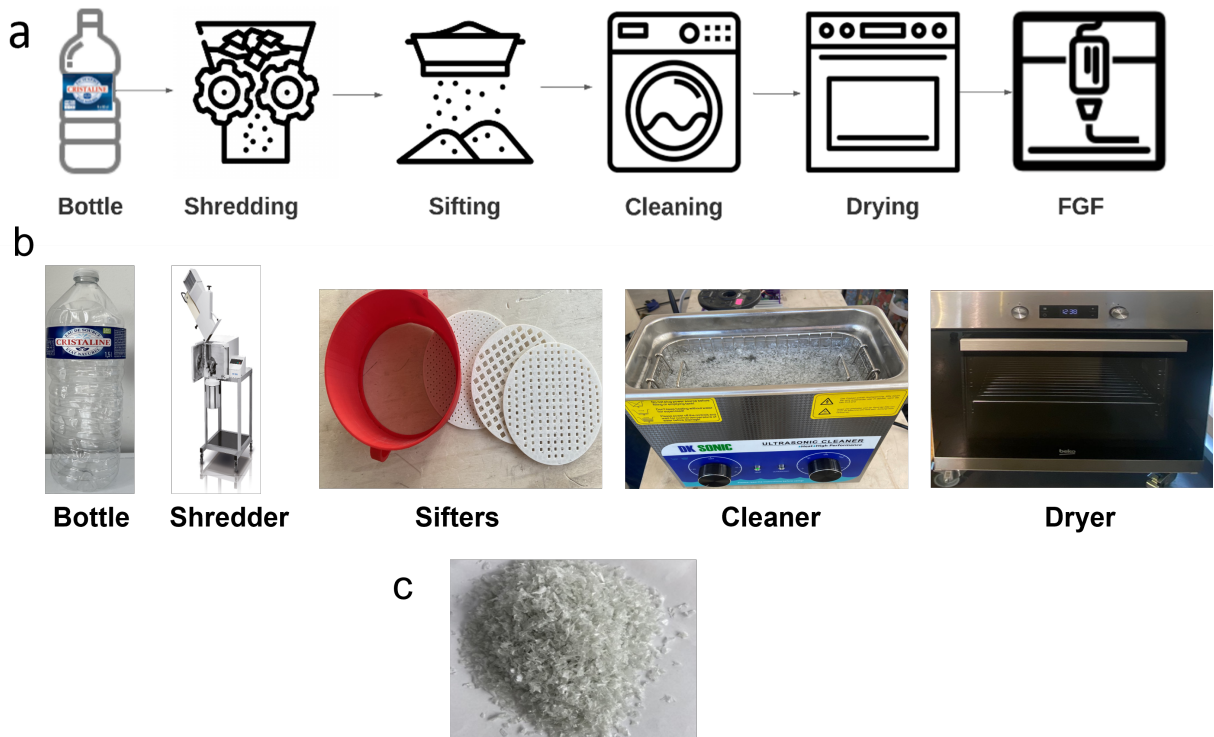


Figure 2: Process steps to prepare the collected material

93 Fourier-transform infrared spectroscopy –FTIR-

94 FTIR spectroscopy was conducted to determine the composition of the bottle and identify any impurities,
95 plasticizers, or additives. The analysis involving testing separate samples of rPET and rHDPE. Additionally,
96 a printed sample of both materials was examined to identify any potential chemical bonding. Each sample
97 was measured at two different points, with three measurements taken at each point. The resulting curves were
98 then normalized and analyzed using Origin Pro 8. The Fourier transform infrared spectra were recorded in
99 the range of 4000 cm^{-1} to 375 cm^{-1} with a resolution of 4 cm^{-1} using a Bruker IFS 66V spectrophotometer.

100 Differential scanning calorimetry –DSC-

101 Differential scanning calorimetry analysis was performed using a DSC-1 Mettler Toledo with STARe software
102 operating under nitrogen atmosphere at heating rate and cooling rate of $10\text{ }^{\circ}\text{C}/\text{min}$. The samples investigated
103 were rPET, rHDPE, and rPET90//rHDPE10. Three cycles were conducted: the first involved heating from
104 $20\text{ }^{\circ}\text{C}$ to $270\text{ }^{\circ}\text{C}$, cooling to $20\text{ }^{\circ}\text{C}$ and reheating to $270\text{ }^{\circ}\text{C}$. The rHDPE sample was analyzed using similar cycles
105 but with the maximum temperature set at $250\text{ }^{\circ}\text{C}$ and the blend was tested at temperatures ranging from
106 -20 to $270\text{ }^{\circ}\text{C}$. The glass transition temperature (T_g) of rPET was determined during the first heating cycle,
107 while the T_g of rPET90//rHDPE10 was determined during the second heating cycle, along with the melting

108 point of all materials. The crystallization temperature (T_c) was determined during the cooling cycle for each
 109 material. The degree of crystallinity (X_c) was calculated from the second cycle for recycled materials and
 110 the first cycle for the blend, as expressed in equation (1) [57], [59]:

$$X_c(\%) = \frac{\Delta H_m}{w \cdot \Delta H_m^\circ} \quad (1)$$

111 Where, ΔH_m is the latent heat of melt, w is the weight percentage of polymer in the blend, and ΔH_m° is
 112 the reference heat of 100% crystalline PET (140 J/g) and HDPE (293 J/g), respectively, provided in the
 113 literature [59], [60].

114 Melt Flow Index –MFI-

115 The melt-flow index (MFI) of rPET90//rHDPE10 flakes was determined using an Instron CEAST MF20.
 116 The analysis was performed using three samples of ~5 g at a temperature of 255 °C with a 2.16 kg weight
 117 following the ASTM D1238 standard. The process was repeated three times. The average value of the three
 118 results was reported in units of $gr/10 \times min.$

119 Density

120 The material's density was calculated as follows: first, the volume was found by measuring the dimensions of
 121 a solid 50x50x50 mm cubic geometry fabricated by injecting rPET90//rHDPE10 flakes into a square mold
 122 with a known volume using an open-source desktop injection machine(Holipress, Holimaker, France). Then,
 123 the model was weighed, and the mass was obtained. Finally, the density was calculated as expressed in
 124 Equation 2. To ensure the accuracy of the test it was performed twice and the average value was reported
 125 in g/cm^3 .

$$\rho = V/m \quad \left[\frac{g}{cm^3} \right] \quad (2)$$

126 Where, ρ is the density, V is the volume, and m the mass.

127 Afterwards, experimental results were compared with the theoretical blend density which could be calculated
 128 by Equation 3.

$$\rho_{12} = \frac{1}{\frac{W_1}{\rho_1} + \frac{W_2}{\rho_2}} \quad \left[\frac{g}{cm^3} \right] \quad (3)$$

129 Where, ρ_{12} is the density of the blend, W_1 and W_2 , the weight fractions of each polymer, ρ_1 and ρ_2 , the
130 theoretical density of each polymer for PET (1.38 g/cm^3) and HDPE 0.93 to 0.97 g/cm^3 [61].

131 **Printing process**

132 **Establishing optimal parameters**

133 Establishing the optimal combinations of parameters is essential for improve the quality and mechanical
134 properties of printed parts [62]. According to [63], particle swarm optimization (PSO) is an accurate and time-
135 effective method for achieving this goal. To optimize the 3-D printing parameters for the rPET90//rHDPE10
136 material in the GigabotX we utilized the open-source PSO Experimenter platform which is available for Linux.
137 The methodology developed by [63] was followed during the optimization. For benchmarking purposes, three
138 artifacts were printed: a line, a plane, and a cube. These artifacts were modeled in CAD software Onshape
139 CAD v1.150 and sliced using Prusaslicer v2.52.0. Figure 3 presents the geometry models and dimensions of
140 the artifacts.

Geometry	Lenght (mm)	width (mm)	height (mm)
Line	200	2	1
Plane	100	100	1
Cube	40	40	40

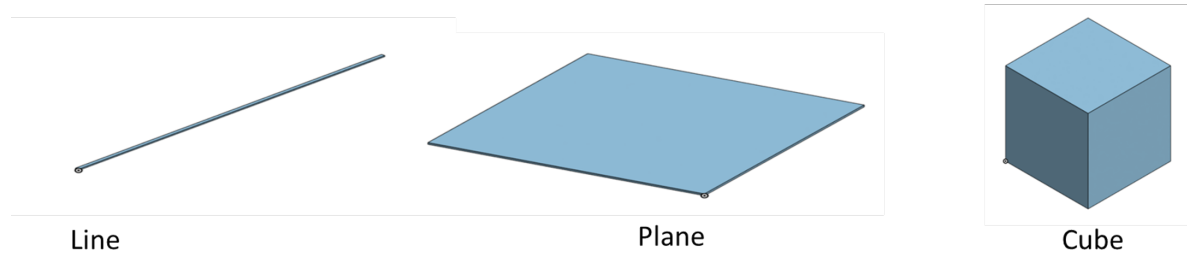


Figure 3: Dimensions and CAD models of the geometries used for parameters optimization.

141 Four parameters were assessed: 1) nozzle temperature, 2) bed temperature, 3) printing speed and 4) extrusion
142 multiplier [64]. The initial parameters for the line are presented in Table 1a while additional parameters were
143 obtained from preliminary experimental work shown in Table 1.b. Finally, the PSO tuning parameters were
144 found in the previous PSO work [63] Table 1.c.

145 **Fused Granular Fabrication –FGF-**

146 To print the obtained raw material, a modified open-source printer with three heat zones (Gigabot XL re:3D,
147 Houston, TX, USA) was utilized as illustrated in Figure 4. The machine is a single screw extrusion-based
148 3-D printer capable of direct printing pellets, flakes, or granules, with a nozzle size of 1.75 mm. For this

Table 1: table 1

(a) Line optimization initial parameters

Variable	Min	Max	Guess	True/False	Description
T1	255	270	260	TRUE	Temperature Zone 1 on GigabotX
Tb	80	90	85	TRUE	Bed temperature
Ps	10	25	15	TRUE	Printing Speed
E	0.5	2	1	FALSE	Extrusion Multiplier

(b) Fixed parameters to perform printing parameters optimization based on PSO

Parameters	Value	Units
Layer height	0.5	mm
Width	2	mm
T2	230	°C
T3	220	°C
Cooling	0	%
Infill density	2	%

(c) Recommended parameters for PSO tuning

Variable	Value	Description
Kv	0.5	The emphasis given to the velocity component
Kp	1.0	The emphasis given to a particle's personal best position
Kg	2.0	The emphasis given to the swarm's group's best position

149 study, a chair was printed to evaluate the material's ability to be 3-D printed and the printer's capability to
 150 produce large objectslike furniture. The ideal parameters determined for the cube geometry were employed
 151 to print the final part.

152 Results and discussion

153 Material characterization

154 Both the polymeric components of the bottle and the blend were characterized and analyzed to determine
 155 their properties using different methods as described in the preceding section.

156 Material particle size analysis (granulometry)

157 Previous studies demonstrated that particles with areas smaller than 22 mm^2 were optimal for printing
 158 without experiencing jamming or under-extrusion problems [11]. However, our experiments revealed that
 159 particles with areas exceeding 10 mm^2 caused clogging in the feeding system and auger screw of the machine.
 160 As a result, granulometry analysis was performed using three different mesh sizes.

161 Figure 5 presents the obtained results, indicating that particles sifted at 5 mm exhibited an average area
 162 similar to the reference. There are, however, particles with areas exceeding 9 mm^2 caused blockages in

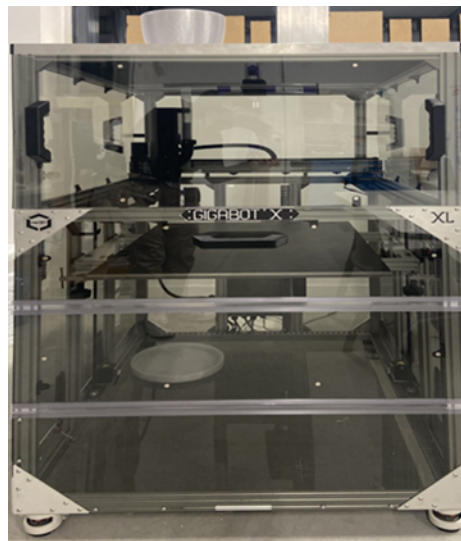


Figure 4: Fused granular fabrication printer Gigabot

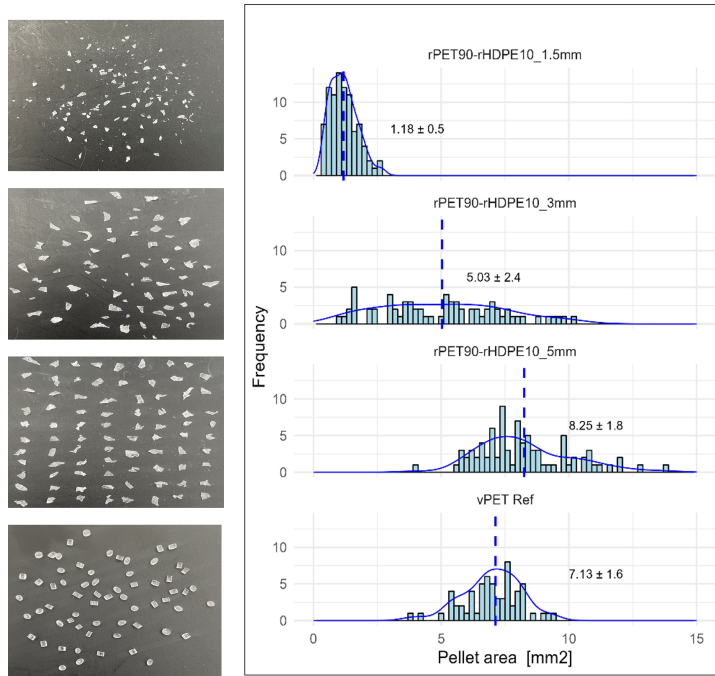


Figure 5: Granulometry analysis

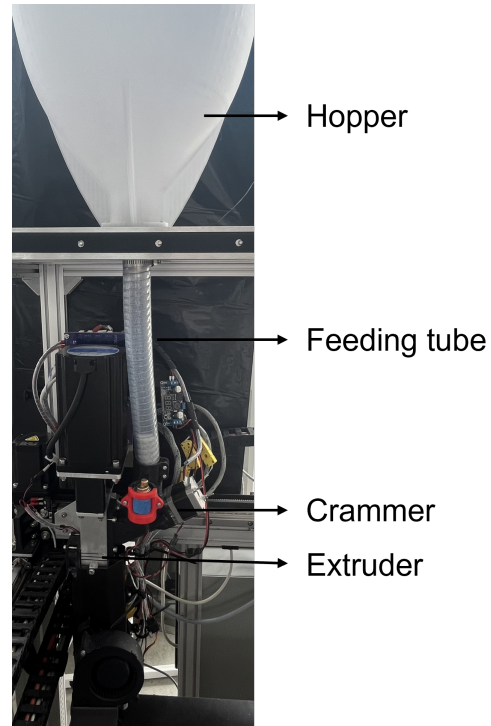


Figure 6: Gigabot feeding system

163 the feeding and extrusion section. Particles sifted to 1.5 mm displayed a distribution ranging from 0 to
164 approximately 3 mm², which was deemed too small for printing purposes. The presence of these small
165 particles can lead to their complete melting in the initial heat zone, thereby impeding the smooth flow of
166 other particles and preventing the necessary pressure for extruding the melted particles further down the
167 screw. Although flakes measuring 3 mm exhibited a more dispersed distribution and slightly smaller area
168 compared to the reference, they were found to be optimal for printing.

169 The final objects, however, still showed under-extrusion issues. To address this problem, a crammer was
170 implemented [55] as presented in Figure 6. The crammer physically pushes particles towards the auger,
171 facilitating their transfer from the feeding tube to the extruder. After the crammer implementation the
172 under-extrusion issues were greatly reduced. It was concluded that flakes with areas ranging from 1.5 mm²
173 to 10 mm² were the most suitable for printing when using a crammer to assist the feeding system.

174 **Chemical analysis from FTIR**

175 Chemical structure information of the materials was obtained using FTIR spectroscopy, which allowed the
176 analysis of the characteristic spectral bands of the polymers.

177 In the case of rPET (bottle) four distinct bands can be observed in Figure 7. The first band, located at
178 1713cm⁻¹ represent the C = O double bond. The second band, at 1240cm⁻¹, corresponds to the C – O
179 single bond ester. The third band, at 1093cm⁻¹, is associated with band the methylene group and vibrations
180 of the ester bond. Lastly, a band at 722cm⁻¹ which represents the CH₂ rocking bending vibration. Similar
181 results were reported in the literature for PET derived from recycled water bottles, soda bottles, and food
182 containers [29].

183 Regarding rHDPE (caps), four characteristic peaks were identified: the C-H functional group bond at
184 2915cm⁻¹ and 2847 cm⁻¹, the primary bending mode of the -CH₂ at 1465 cm⁻¹ and the CH₂ rocking
185 bending vibration at 729 cm⁻¹. The results obtained confirmed the chemical structures of the starting mate-
186 rials. Additionally, no other indicative resonances, apart from those associated with the polymer structures
187 were detected. This leads to the conclusion that there were no significant amounts of additives or plasticizers
188 present in either of the samples. Moreover, the spectrum of the printed blend (rPET90//rHDPE10) exhibited
189 identical characteristic peaks to those observed in the bottle, thus confirming the predominant presence of
190 PET. There are, however, noticeable differences between 1000 cm⁻¹ and 720 cm⁻¹ as well as in the C-H
191 bond (2915 cm⁻¹ and 2847 cm⁻¹ peaks), which confirm the presence of HDPE (cap). The observed shift can
192 be attributed to interactions between the two materials.

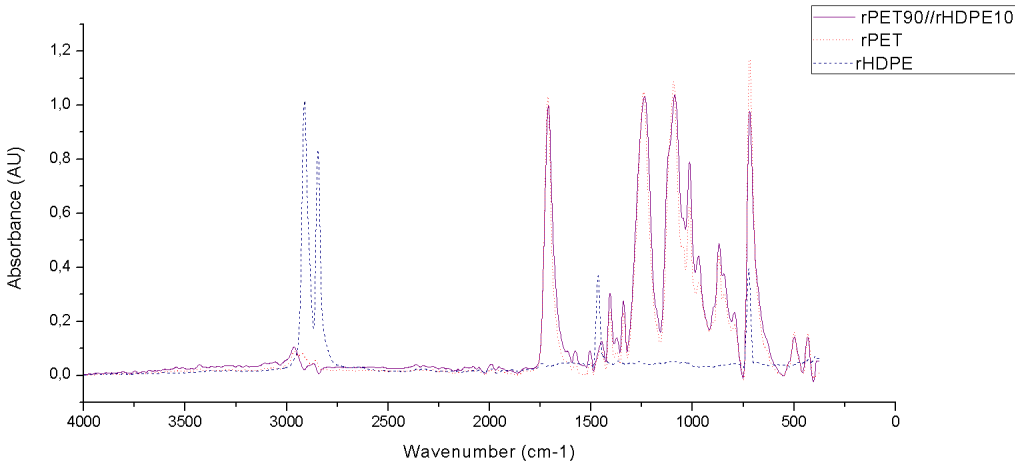
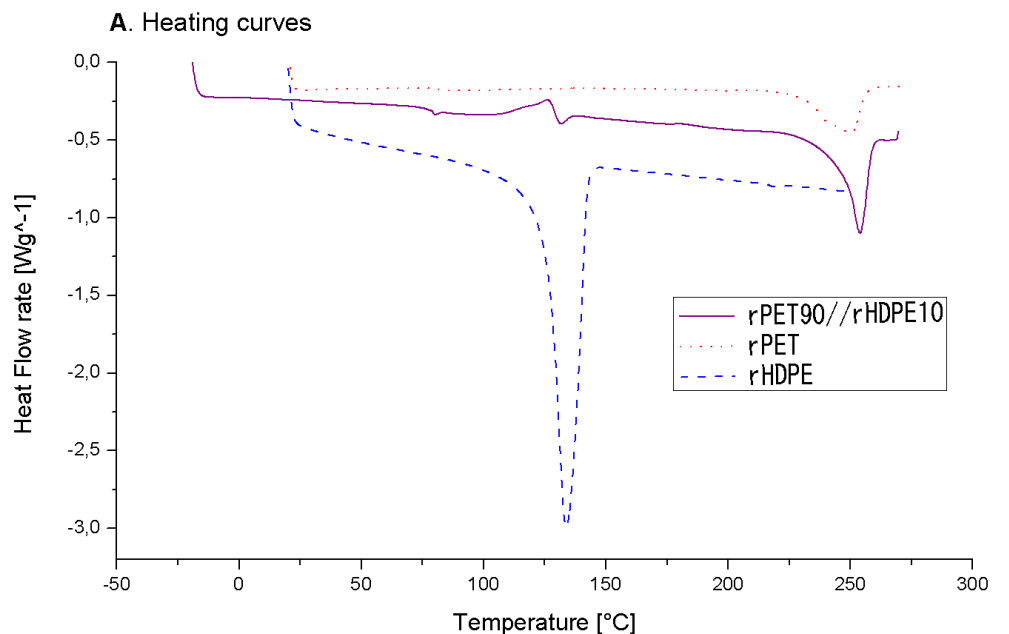


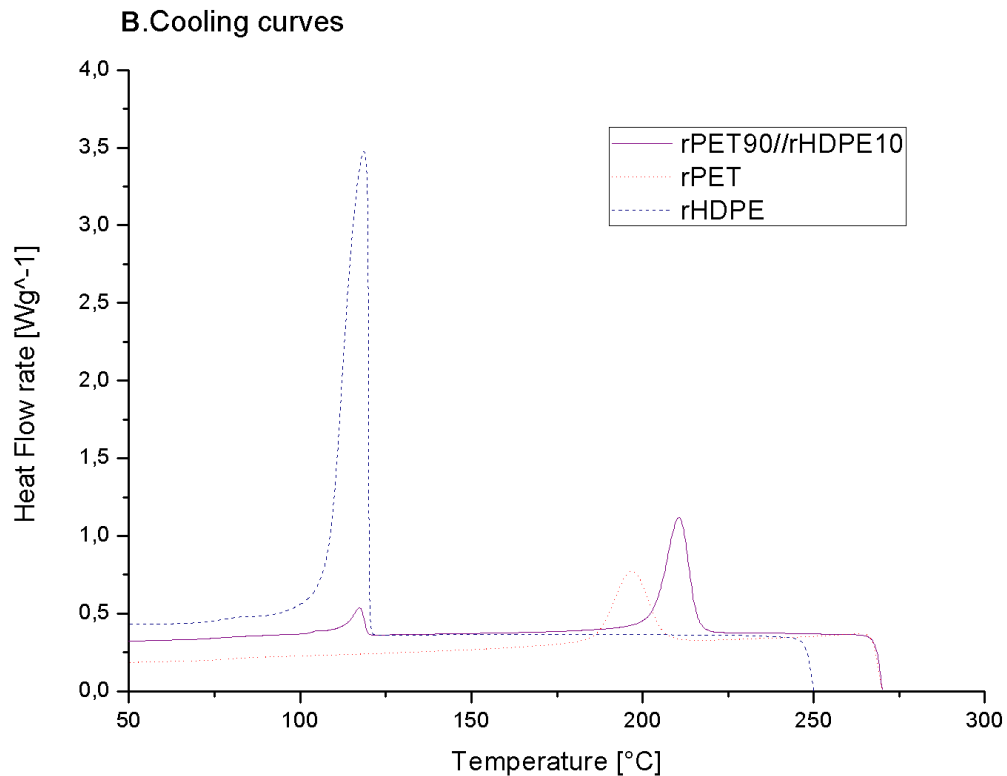
Figure 7: FTIR spectra of rPET, rHDPE, and their blend

¹⁹³ **Thermal analysis DSC**

¹⁹⁴ The thermal properties of both recycled materials and their blend were characterized using DSC to establish
¹⁹⁵ a baseline for optimizing process parameters of 3-D printing.
¹⁹⁶ Two distinct endothermic peaks are observed in the representative heating and cooling thermograms shown in
¹⁹⁷ Figure 8, for the printed blend sample. These peaks are associated with the fusion of the crystalline fractions
¹⁹⁸ of rHDPE and rPET, providing confirmation of the immiscibility of both materials. Moreover, the enthalpy
¹⁹⁹ of fusion and crystallization of the rHDPE in the blend is significantly reduced, which can be attributed to
²⁰⁰ the low percentage of HDPE present in the blend. Furthermore, the presence of a cold crystallization peak
²⁰¹ in the blend, but not in the individual polymers, suggests an interaction between the two polymers. It is
²⁰² possible that the rHDPE acts as a nucleating agent in this interaction. Table 2 lists the thermal properties of
²⁰³ rPET, rHDPE and rPET90//rHDPE10. The melting points of rHDPE and rPET are 131.7 °C and 249.9 °C,
²⁰⁴ respectively, which align with previous findings in the literature [30], [65], [66]. It is observed that the melting
²⁰⁵ and crystallization temperature of rPET increased, while that of rHDPE slightly decreased. Furthermore,
²⁰⁶ the crystallization of rPET was found to be somewhat affected by the presence of rHDPE, resulting in a 3.5%
²⁰⁷ increase in degree of crystallization. This can be attributed to the rHDPE acting as a germination point for
²⁰⁸ crystallization [30]. The slight changes in the fusion-crystallization temperatures and degree of crystallinity
²⁰⁹ of rPET indicate an interaction of both polymers.



(a) Heating curves



(b) Cooling curve

Figure 8: DSC thermograms of recycled materials and blends ¹³

Table 2: Thermal analysis of rPET, rHDPE, and their blend

Sample	Glass transition		Melting		Crystallization			% Crystallinity
	Tg (°C)		Tm (°C)	ΔHm (J/g)	Tc (°C)	ΔHc (J/g)	ΔHcc (J/g)	
rPET	82		249.9	32.3	196.7	33.3	-	23.1
rHDPE	-		133.8	172	118.7	158.2	-	58.7
rPET90/rHDPE10	77 / -		254/131.7	40.3/1.30	210.6/117.4	37.9/6.7	6.8	26.6 / 18.8

210 Rheology MFI

211 The melt flow index of the flakes was determined, enabling a fast and practical screening of the viscosity of
 212 the material. Based on the DSC results, the initial temperature for the MFI test was 250°C. However, the
 213 material did not flow reliably at this temperature, so it was increased by 5°C to enable the determination of
 214 the melt flow index of the rPET90//rHDPE10 blend. A temperature of 260°C was also tested, however, the
 215 material flowed too rapidly, making difficult to obtain reliable measurements. The MFI tests were performed
 216 three times and the results for the rPET90//rHDPE10 blend showed medium MFI of 39.4 ± 2.4 g/10min. This
 217 value is consistent with similar values reported in the literature for rPET [67]–[69]. This result suggest that
 218 addition of low percentage of HDPE does not significantly impact the MFI value of rPET. Since the material
 219 flowed at a temperature of 255°C in the MFI test, this temperature was used as the input temperature for
 220 optimizing the parameters of the 3-D printer.

221 Density

222 The density provides valuable information for estimating the cost, material usage, time consumption, and
 223 weight of the printed object in the slicer. This information is useful to determine the accurate printing
 224 parameters using the PSO experimenter, as the fitness of the object is calculated based on its dimensional
 225 accuracy and weight. Hence, density plays a significant role in determining the weight of the geometries.

226 After conducting calculations and measuring the rPET90//rHDPE10 injected object, it was determined that
 227 the density of the material is 1.13 g/cm^3 . The inclusion of HDPE in the matrix polymer resulted in a slight
 228 decrease in density, which is a common occurrence when a polymer is mixed with a lower-density polymer.
 229 However, if we consider a PET/HDPE blend with a mass ratio of 90/10, the calculated theoretical density
 230 would be 1.32 g/cm^3 . The observed decrease of 14% in the results could be attributed to factors, such as
 231 experimental conditions and manual measurements.

232 Particle swarm optimization (PSO) Experimenter

233 Geometries were 3-D printed by adjusting the parameters using the PSO Experimenter software. The fit-
 234 ness function is defined by the weighted sum of the dimensional measurements (length, width, height, and

235 weight) of the printed object. A fitness value below 0.1 was consider desirable. In the software five particles
236 were established for each iteration, resulting in five different parameter combinations being printed in each
237 iteration.

238 After six iterations and a total of thirty lines printed, the first geometry (line) achieved a fitness value of less
239 than 0.1. The optimal parameters for this geometry are listed in column two of Table 3 and images of the
240 resulting geometries are illustrated in Figure 9 .

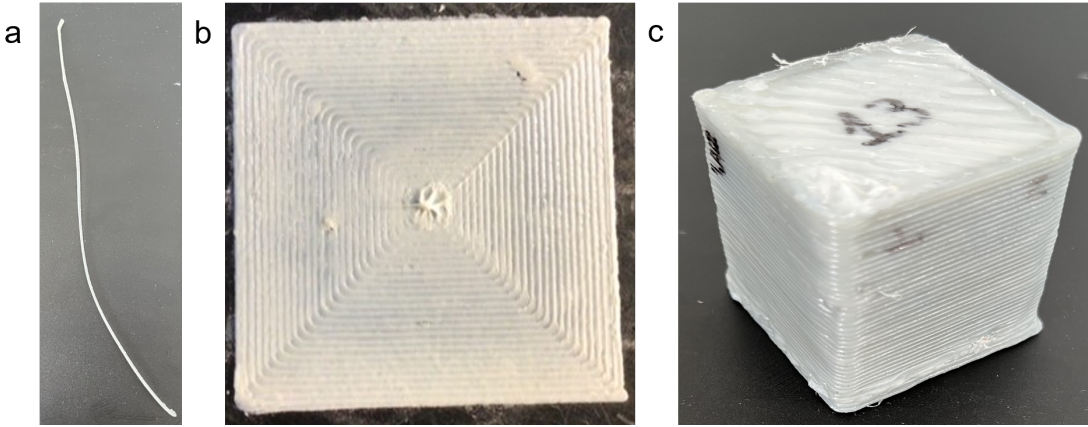


Figure 9: Images of the resulting geometries a) line, b) plane, c) cube

241 Afterwards, these parameters were used as initial guesses for plane geometry, which achieved the desired
242 fitness in the first iteration. Similarly, cubes were printed using the plane ideal parameter as the initial
243 guess, and optimal parameters, were found in the first iteration. The results showed a significant decrease
244 in printing speed, as the geometry complexity increased. Moreover, the cube geometry required a higher
245 extrusion multiplier to fill gaps and overcome under-extrusion problems. The optimization of parameters
246 for the three geometries took approximately 10h reducing the experimental time, compared to conventional
247 methods. According to [63], this experimentation time can be reduced by 97%. Indeed, the effectiveness of
248 PSO in finding global optimum parameters is high, especially in cases with a large or complex design space
249 [70], [71].

250 Additionally, PSO converge to optimum solutions with fewer iterations than DoE methods [72]. Combining
251 PSO with other meta-heuristic methods has demostrated higher ability to predict and optimize parameters
252 (e.g. minimize surface roughness[73], compressive strength and porosity of scaffolds [74],and mechanical prop-
253 erties[75]). However, DoE methods are still widely used as they provide insight into the effects of individual
254 design parameters and their interactions while the ability to find interaction between the variables is not pos-
255 sible using PSO. In the beginning of optimization experiments, the understanding the process technique and
256 function settings might be complex. The methodology used in this study, however, was easy to implement

Table 3: Ideal printing parameters for fused granule fabrication of waste PET and HDPE blend made from shredded whole plastic water bottles

Variable	Line value	Planes value	Cube value	Δ	Units
T1	258	263	264	6 ±3.2	°C
Tb	86	82	84	4±2	°C
Ps	21	14	10	11±5.6	mm/s
E	1.07	0.87	1.32	0.5±0.3	-

and the software used was free, open source, and user-friendly, which reduced the initial difficulty. Therefore, PSO was demonstrated to be an effective and highly accurate prediction technique for finding the initial optimum parameters for rPET90//rHDPE10 material for FGF/FPF.

Based on the result, it is evident that the optimal parameters for printing may vary depending on the object and each parameter has its own variation. One possible hypothesis is that the geometry of the object could influence the assignment of parameters and this effect might be more noticeable in large printings, yet further investigation is required to confirm this hypothesis. There are several physical mechanisms at play that are expected to alter the optimal printing parameters based on size and geometry of the object. For example, the cooling time and temperature history of a voxel will depend on the geometry of the printed object [76]. Thus, to maintain a consistent thermal history the printing parameters must be adjusted as the geometry changes. This thermal history can also have more subtle effects, such as impacting the degree of crystallization even in the case of PLA [77].

In addition, the effects of material extrusion are magnified with scale, including the impact of thermal expansion and contraction. Small changes in contraction during cooling may cause acceptable distortions for small prints, but these are magnified for larger prints (e.g. causing deformation and in the worst cases delamination or loss of bed adhesion)[78]. Although, [79] showed the obstacles and possible solutions of the large-scale AM according to the way the parts are designed the incidence of the geometry in the printing parameters needs far more detailed future studies. Specifically better models for mapping 3-D printing parameter optimization of small printed objects to large-volume objects are needed.

Functional object print

The final parameters for print the case study product were determined based on the ideal paraeters found for the cube geometry.However, the print speed was adjusted to decrease the printing time and prevent delamination. This adjustment was made in accordance with the PSO results, which indicated that the material can be printed at a speed range of 10 to 20 mm/s. Increasing the printing speed reduces the cooling time between the layers,thereby minimizing the risk of delamination [79], This is particularly important for

²⁸² larger objects, as delamination tends to be more pronounced in such cases.

²⁸³ The Gigabot X successfully produced a piece of furniture from multi-material recycled water bottles that

²⁸⁴ included mixing HDPE and PET as shown in Figure 10 a.

²⁸⁵ The printing quality is acceptable as a prototype, proving the machine's capacity to print large-scale functional

²⁸⁶ objects. The chair was able to comfortably hold a child with a mass of 20 kg, as shown in Figure 10 f. However,

²⁸⁷ further evaluation is needed for the material used in the printing process. the printed object showed weak

²⁸⁸ bond strength between the adjacent layers resulting in delamination, as seen in Figure 10 b . This could

²⁸⁹ be attributed to the difference in chemical properties of the materials, their immiscibility [80], [81], high

²⁹⁰ crystallinity [82] and the large volume of the object as delamination issues were more prominent during

²⁹¹ the printing of the chair compared to the parameters optimization process. The delamination observed in

²⁹² larger objects can be attributed to the rapid cooling of the layers before the material is once again deposited.

²⁹³ This is in contrast to cube printing, where the smaller surface area allows better layer adhesion before

²⁹⁴ complete cooling. Even popular 3-D printing materials like PLA can be affected by this issue, as observed

²⁹⁵ from the print surface [77]. To address the delamination problem and improve material properties, the

²⁹⁶ addition of agents that reduce could be beneficial [83]–[85]. This can enhance interfacial bonds through

²⁹⁷ polymer modification [86] and viscosity reduction [87]. Additionally, we observed printing warping problems

²⁹⁸ (Figure 10 c), which are likely caused by the high crystallization rates of HDPE. we tested the use of Magigoo

²⁹⁹ adhesive (Thought3D Ltd., Paola, Malta) and the addition of a brim to improve bed adhesion, yet these

³⁰⁰ solutions did not completely resolve the problem. A previous study showed that the use of a building plate

³⁰¹ made of thermoplastic elastomer SEBS allowed the adhesion of the plastic and facilitated easy detachment of

³⁰² the printed object without any breakage or damage **[schirmeister2019.This?]** suggests a potential solution

³⁰³ that should be further evaluated in future work. Another visible issue present in the close angles of the

³⁰⁴ printed object was the shrinkage (Figure 10 d) which occurs during solidification and particularly upon

³⁰⁵ polymer crystallization. Moreover, it is well-known that PET has hygroscopic tendencies and easily absorbs

³⁰⁶ moisture from the temperature, which makes it difficult to extrude [67]. As result, it is likely to break down

³⁰⁷ in the presence of water, lowering the quality of the print. Prior to printing the chair some samples exhibited

³⁰⁸ brittle behavior and void formation therefore, the material was consistently dried and the hopper was kept

³⁰⁹ closed to prevent moisture from entering the environment. These measures helped to ensure a more suitable

³¹⁰ material for printing. Additionally, there are visible vibration and ringing problems (Figure 10 e) caused by

³¹¹ the machine upgrades. Both acceleration and jerk (the maximum value of instantaneous speed change) require

³¹² finer tuning to resolve these issues.

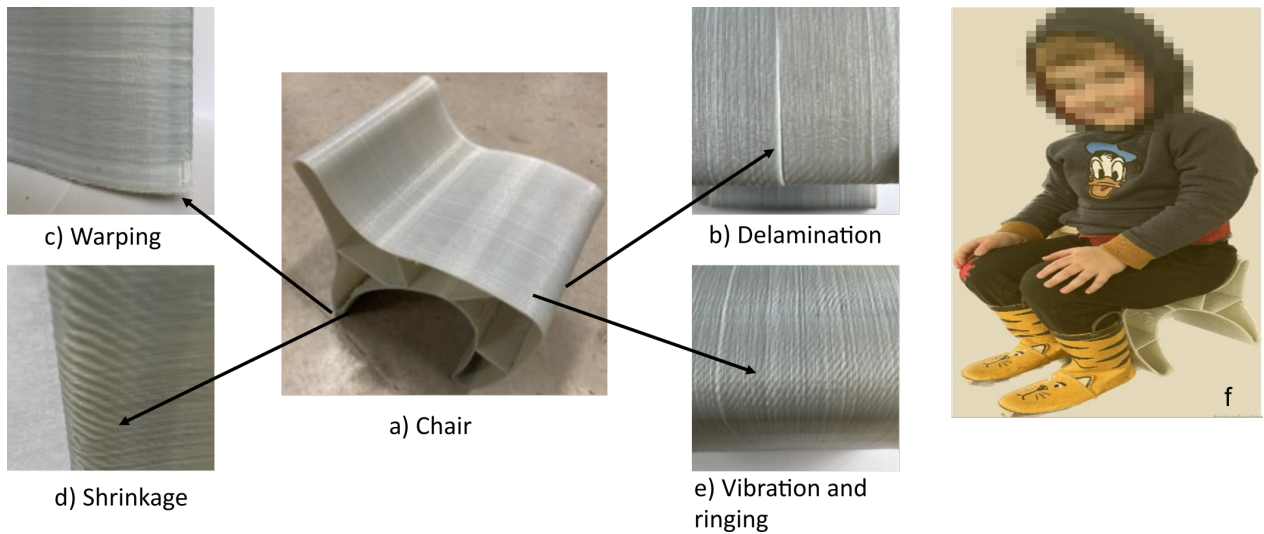


Figure 10: Finished children's chair and printing issues

313 Cost and environmental impact

314 The printing process took 10 hours and the printed object weighs 840 grams. Due to the found optimized
 315 speed being low, the printing rate (grams per hour) is low considering the machine that pellet printers have
 316 a typical throughput of 220 g to 9 kg per hour. To improve the printing time, upgrading the the extruder
 317 motor to a more powerful would be benefitial. Besides, the energy required for 10 hours of 3-D printing was
 318 found to be 6 kW-hr resulting in a production cost of ~1.2 € in function of the electricity cost in France, and
 319 does not include the material cost, as the bottles used were obtained from post-consumer waste. When labor
 320 costs are not included, the price was significant reduced (~88%) compared to the low-cost options available
 321 in the market.

322 The economics of fabricating the case study product remained competitive even when using recycled plastic
 323 pellets or shreds, which are available on the market for prices ranging from 1-10 €/kg. However, it is important
 324 to note that labor, maintenance, and machine devaluation were not considered in the final price. These factors
 325 should be considered in future work to ensure a comprehensive economic evaluation.

326 Regarding the environmental impact, this study does not evaluate the entire life cycle of the printed object.
 327 However, various scientific studies have already shown the feasibility of distributed recycling [17], [88]. A
 328 comparison between conventional and distributed manufacturing in terms of energy consumption and emis-
 329 sions has been conducted [89]. Other studies have examined the environmental performance of AM [90], [91]
 330 and the appearance of DRAM as a source of raw material for diverse 3-D printers coming from post-consumer
 331 plastic waste in the form of either filament [27], [92]–[94] or granules [52].

332 Additionally, [95] have developed a comprehensive life cycle assessment of a DRAM system focusing on the
333 production of PLA filament, comparing virgin and recycled materials. The findings of their environmental
334 analysis revealed a analysis revealed a reduction of approximately 97% in the production impacts, including
335 climate change, fossil depletion, water depletion, and potential eutrophication, when using recycled filament
336 as opposed to virgin filament. It is important to note that these results are subject to the energy supply and
337 might vary depending on the geographical location.

338 Conclusion and future work

339 This study examined the feasibility of using mixed post-consumer waste as a feedstock material for direct 3-D
340 printing without the need of compatibilization. The results demostrated the potential of mixing solid waste
341 plastics (PET/HDPE) to be used as feedstock material, as evidenced by successfully printing a water bottle
342 using two incompatible polymers from the cap and body of the bottle. Additionally, the results found that
343 a large-scale FGF 3-D printer was capable of producing cost-effective functional object using these mixed
344 waste PET/HDPE plastics. However, further research is necessary to analyze the mechanical properties of
345 the material and explore the use of compatibilizers that can enhance the interphase tension between plastics
346 and reduce their crystallinity. These measures could potentially improve and enhance the properties of both
347 the material and the 3-D printed parts.

348 These considerations become increasingly important as the size of the 3-D printed part increases. The
349 improvement of the material science of this approach can also offer an opportunity to improve the quality of
350 the printing time, reduce energy consumption of the machine, and improve the economic viability of DRAM
351 using mixed plastic waste.

352 In addition, future work could assess the different combinations or blends of commodity plastics with or with-
353 out the use of compatibilizers, to determine their printability. This investigation could lead ti the elimination
354 of the selection/sorting process. In the same way, the development of a methodology that ensure process
355 reproducibility, even in areas with limited infrastructure opens up the potential for plastic revalorization
356 using DRAM.

357 Declaration of competing

358 The authors declare that they have no known competing financial interests or personal relationships that
359 could have appeared to influence the work reported in this paper.

³⁶⁰ **Acknowledgments**

³⁶¹ This project has received funding from the European Union’s Horizon 2020 research and innovation program
³⁶² under grant agreement No 869952. The authors thank the LUE program for the financing of the thesis, the
³⁶³ Lorraine Fab Living lab platform and the Thompson endowment.

364 References

- 365 [1] N. Evode, S. A. Qamar, M. Bilal, D. Barceló, and H. M. N. Iqbal, "Plastic waste and its management
strategies for environmental sustainability," *Case Studies in Chemical and Environmental Engineering*,
vol. 4, p. 100142, Dec. 2021, doi: [10.1016/j.cscee.2021.100142](https://doi.org/10.1016/j.cscee.2021.100142).
- 366 [2] E. MacArthur, "Beyond plastic waste," *Science*, vol. 358, no. 6365, pp. 843–843, Nov. 2017, doi:
[10.1126/science.aaq6749](https://doi.org/10.1126/science.aaq6749).
- 367 [3] R. Geyer, "Chapter 2 - Production, use, and fate of synthetic polymers," in *Plastic Waste and Recycling*,
T. M. Letcher, Ed., Academic Press, 2020, pp. 13–32. doi: [10.1016/B978-0-12-817880-5.00002-5](https://doi.org/10.1016/B978-0-12-817880-5.00002-5).
- 368 [4] J. Soares, I. Miguel, C. Venâncio, I. Lopes, and M. Oliveira, "Public views on plastic pollution:
Knowledge, perceived impacts, and pro-environmental behaviours," *Journal of Hazardous Materials*,
vol. 412, p. 125227, Jun. 2021, doi: [10.1016/j.jhazmat.2021.125227](https://doi.org/10.1016/j.jhazmat.2021.125227).
- 369 [5] J. Siltaloppi and M. Jähi, "Toward a sustainable plastics value chain: Core conundrums and emerging
solution mechanisms for a systemic transition," *Journal of Cleaner Production*, vol. 315, p. 128113,
Sep. 2021, doi: [10.1016/j.jclepro.2021.128113](https://doi.org/10.1016/j.jclepro.2021.128113).
- 370 [6] R. Geyer, J. R. Jambeck, and K. L. Law, "Production, use, and fate of all plastics ever made." *Science
Advances*, vol. 3, no. 7, p. e1700782, 2017, doi: [10.1126/sciadv.1700782](https://doi.org/10.1126/sciadv.1700782).
- 371 [7] F. A. Cruz Sanchez, H. Boudaoud, M. Camargo, and J. M. Pearce, "Plastic recycling in additive
manufacturing: A systematic literature review and opportunities for the circular economy," *Journal
of Cleaner Production*, vol. 264, p. 121602, Aug. 2020, doi: [10.1016/j.jclepro.2020.121602](https://doi.org/10.1016/j.jclepro.2020.121602).
- 372 [8] S. C. Dertinger *et al.*, "Technical pathways for distributed recycling of polymer composites for dis-
tributed manufacturing: Windshield wiper blades," *Resources, Conservation and Recycling*, vol. 157,
p. 104810, Jun. 2020, doi: [10.1016/j.resconrec.2020.104810](https://doi.org/10.1016/j.resconrec.2020.104810).
- 373 [9] C. Baechler, M. DeVuono, and J. M. Pearce, "Distributed recycling of waste polymer into
RepRap feedstock," *Rapid Prototyping Journal*, vol. 19, no. 2, pp. 118–125, Jan. 2013, doi:
[10.1108/13552541311302978](https://doi.org/10.1108/13552541311302978).
- 374 [10] S. Zhong and J. M. Pearce, "Tightening the loop on the circular economy: Coupled distributed
recycling and manufacturing with recyclebot and RepRap 3-D printing," *Resources, Conservation
and Recycling*, vol. 128, pp. 48–58, Jan. 2018, doi: [10.1016/j.resconrec.2017.09.023](https://doi.org/10.1016/j.resconrec.2017.09.023).
- 375 [11] A. L. Woern, J. R. McCaslin, A. M. Pringle, and J. M. Pearce, "RepRapable Recyclebot: Open source
3-D printable extruder for converting plastic to 3-D printing filament," *HardwareX*, vol. 4, p. e00026,
Oct. 2018, doi: [10.1016/j.hwx.2018.e00026](https://doi.org/10.1016/j.hwx.2018.e00026).
- 376 [12] S. Ford and M. Despesesse, "Additive manufacturing and sustainability: An exploratory study of the
advantages and challenges," *Journal of Cleaner Production*, vol. 137, pp. 1573–1587, Nov. 2016, doi:
[10.1016/j.jclepro.2016.04.150](https://doi.org/10.1016/j.jclepro.2016.04.150).
- 377 [13] M. Despesesse *et al.*, "Unlocking value for a circular economy through 3D printing: A research
agenda," *Technological Forecasting and Social Change*, vol. 115, pp. 75–84, Feb. 2017, doi:
[10.1016/j.techfore.2016.09.021](https://doi.org/10.1016/j.techfore.2016.09.021).
- 378 [14] E. Petersen, R. Kidd, and J. Pearce, "Impact of DIY Home Manufacturing with 3D Printing on the
Toy and Game Market," *Technologies*, vol. 5, no. 3, p. 45, 2017, doi: [10.3390/technologies5030045](https://doi.org/10.3390/technologies5030045).
- 379 [15] N. Gallup, J. K. Bow, and J. M. Pearce, "Economic Potential for Distributed Manufacturing of
Adaptive Aids for Arthritis Patients in the U.S." *Geriatrics*, vol. 3, no. 4, p. 89, Dec. 2018, doi:
[10.3390/geriatrics3040089](https://doi.org/10.3390/geriatrics3040089).

- 395 [16] J. Pearce and J.-Y. Qian, "Economic Impact of DIY Home Manufacturing of Consumer Products with
396 Low-cost 3D Printing from Free and Open Source Designs," *European Journal of Social Impact and
Circular Economy*, vol. 3, no. 2, pp. 1–24, Jul. 2022, doi: [10.13135/2704-9906/6508](https://doi.org/10.13135/2704-9906/6508).
- 397 [17] P. Santander, F. A. Cruz Sanchez, H. Boudaoud, and M. Camargo, "Closed loop supply chain
network for local and distributed plastic recycling for 3D printing: A MILP-based optimization
approach," *Resources, Conservation and Recycling*, vol. 154, p. 104531, Mar. 2020, doi:
[10.1016/j.resconrec.2019.104531](https://doi.org/10.1016/j.resconrec.2019.104531).
- 398 [18] M. A. Kreiger, M. L. Mulder, A. G. Glover, and J. M. Pearce, "Life cycle analysis of distributed
recycling of post-consumer high density polyethylene for 3-D printing filament," *Journal of Cleaner
Production*, vol. 70, pp. 90–96, May 2014, doi: [10.1016/j.jclepro.2014.02.009](https://doi.org/10.1016/j.jclepro.2014.02.009).
- 400 [19] A. Romani, V. Rognoli, and M. Levi, "Design, Materials, and Extrusion-Based Additive Manufacturing
in Circular Economy Contexts: From Waste to New Products," *Sustainability*, vol. 13, no. 13, p. 7269,
401 Jan. 2021, doi: [10.3390/su13137269](https://doi.org/10.3390/su13137269).
- 402 [20] R. Jones *et al.*, "RepRap – the replicating rapid prototyper," *Robotica*, vol. 29, no. 1, pp. 177–191,
403 Jan. 2011, doi: [10.1017/S026357471000069X](https://doi.org/10.1017/S026357471000069X).
- 404 [21] E. Sells, Z. Smith, S. Bailard, A. Bowyer, and V. Olliver, "RepRap: The Replicating Rapid Prototyper
- maximizing customizability by breeding the means of production," in *Handbook of Research in Mass
Customization and Personalization*, vol. 1, F. T. Piller and M. M. Tseng, Eds., World Scientific, 2009,
405 pp. 568–580.
- 406 [22] A. Bowyer, "3D Printing and Humanity's First Imperfect Replicator," *3D Printing and Additive
Manufacturing*, vol. 1, no. 1, pp. 4–5, Mar. 2014, doi: [10.1089/3dp.2013.0003](https://doi.org/10.1089/3dp.2013.0003).
- 408 [23] J. P. Rett, Y. L. Traore, and E. A. Ho, "Sustainable Materials for Fused Deposition Modeling 3D
Printing Applications," *Advanced Engineering Materials*, vol. 23, no. 7, p. 2001472, 2021, doi:
[10.1002/adem.202001472](https://doi.org/10.1002/adem.202001472).
- 410 [24] J. Pakkanen, D. Manfredi, P. Minetola, and L. Iuliano, "About the Use of Recycled or Biodegradable
Filaments for Sustainability of 3D Printing," vol. 68, G. Campana, R. J. Howlett, R. Setchi, and B.
Cimatti, Eds., Cham: Springer International Publishing, 2017, pp. 776–785. doi: [10.1007/978-3-319-57078-5_73](https://doi.org/10.1007/978-3-319-57078-5_73).
- 412 [25] F. A. Cruz Sanchez, H. Boudaoud, S. Hoppe, and M. Camargo, "Polymer recycling in an open-source
additive manufacturing context: Mechanical issues," *Additive Manufacturing*, vol. 17, pp. 87–105,
414 Oct. 2017, doi: [10.1016/j.addma.2017.05.013](https://doi.org/10.1016/j.addma.2017.05.013).
- 416 [26] I. Anderson, "Mechanical Properties of Specimens 3D Printed with Virgin and Recycled Polylactic
Acid," *3D Printing and Additive Manufacturing*, vol. 4, no. 2, pp. 110–115, Jun. 2017, doi:
[10.1089/3dp.2016.0054](https://doi.org/10.1089/3dp.2016.0054).
- 418 [27] M. I. Mohammed *et al.*, "A low carbon footprint approach to the reconstitution of plastics into
3D-printer filament for enhanced waste reduction," *KnE Engineering*, pp. 234–241, Feb. 2017, doi:
[10.18502/keg.v2i2.621](https://doi.org/10.18502/keg.v2i2.621).
- 420 [28] M. I. Mohammed, A. Das, E. Gomez-Kervin, D. Wilson, and I. Gibson, "EcoPrinting: Investigating the
Use of 100% Recycled Acrylonitrile Butadiene Styrene (ABS) for Additive Manufacturing," University
of Texas at Austin, 2017.
- 422 [29] N. E. Zander, M. Gillan, and R. H. Lambeth, "Recycled polyethylene terephthalate as a new
FFF feedstock material," *Additive Manufacturing*, vol. 21, pp. 174–182, May 2018, doi:
[10.1016/j.addma.2018.03.007](https://doi.org/10.1016/j.addma.2018.03.007).

- 422
- 423 [30] J. Vaucher, A. Demongeot, V. Michaud, and Y. Leterrier, "Recycling of Bottle Grade PET: Influence
424 of HDPE Contamination on the Microstructure and Mechanical Performance of 3D Printed Parts,"
Polymers, vol. 14, no. 24, p. 5507, Jan. 2022, doi: [10.3390/polym14245507](https://doi.org/10.3390/polym14245507).
- 425 [31] S. Chong, G.-T. Pan, M. Khalid, T. C.-K. Yang, S.-T. Hung, and C.-M. Huang, "Physical Characteriza-
426 tion and Pre-assessment of Recycled High-Density Polyethylene as 3D Printing Material," *Journal
427 of Polymers and the Environment*, vol. 25, no. 2, pp. 136–145, Jun. 2017, doi: [10.1007/s10924-016-0793-4](https://doi.org/10.1007/s10924-016-0793-4).
- 428 [32] V. Gaikwad, A. Ghose, S. Cholake, A. Rawal, M. Iwato, and V. Sahajwalla, "Transformation of E-
429 Waste Plastics into Sustainable Filaments for 3D Printing," *ACS Sustainable Chemistry & Engineering*,
430 vol. 6, no. 11, pp. 14432–14440, Nov. 2018, doi: [10.1021/acssuschemeng.8b03105](https://doi.org/10.1021/acssuschemeng.8b03105).
- 431 [33] A. M. Pringle, M. Rudnicki, and J. M. Pearce, "Wood Furniture Waste-Based Recycled 3-D Printing
432 Filament," *Forest Products Journal*, vol. 68, no. 1, pp. 86–95, Jan. 2018, doi: [10.13073/FPJ-D-17-00042](https://doi.org/10.13073/FPJ-D-17-00042).
- 433 [34] S. K. Lösche, J. Mai, G. Proust, and A. Brambilla, "Microtimber: The Development of a 3D Printed
434 Composite Panel Made from Waste Wood and Recycled Plastics," *Digital Wood Design*, vol. 24, pp.
435 827–848, 2019, doi: [10.1007/978-3-030-03676-8_33](https://doi.org/10.1007/978-3-030-03676-8_33).
- 436 [35] I. A. Carrete, P. A. Quiñonez, D. Bermudez, and D. A. Roberson, "Incorporating Textile-Derived Cel-
437 lulose Fibers for the Strengthening of Recycled Polyethylene Terephthalate for 3D Printing Feedstock
438 Materials," *Journal of polymers and the environment*, 2021.
- 439 [36] N. E. Zander, M. Gillan, Z. Burckhard, and F. Gardea, "Recycled polypropylene blends as
440 novel 3D printing materials," *Additive Manufacturing*, vol. 25, pp. 122–130, Jan. 2019, doi:
441 [10.1016/j.addma.2018.11.009](https://doi.org/10.1016/j.addma.2018.11.009).
- 442 [37] B. L. Savonen, T. J. Mahan, M. W. Curtis, J. W. Schreier, J. K. Gershenson, and J. M. Pearce,
443 "Development of a Resilient 3-D Printer for Humanitarian Crisis Response," *Technologies*, vol. 6, no.
444 1, p. 30, Mar. 2018, doi: [10.3390/technologies6010030](https://doi.org/10.3390/technologies6010030).
- 445 [38] L. Corsini, C. B. Aranda-Jan, and J. Moultrie, "The impact of 3D printing on the humanitarian supply
446 chain," 2022, doi: [10.17863/CAM.51226](https://doi.org/10.17863/CAM.51226).
- 447 [39] S. Lipsky, A. Przyjemska, M. Velasquez, and J. Gershenson, "3D Printing for Humanitarian Relief:
448 The Printer Problem," in *2019 IEEE Global Humanitarian Technology Conference (GHTC)*, Oct. 2019,
449 pp. 1–7. doi: [10.1109/GHTC46095.2019.9033053](https://doi.org/10.1109/GHTC46095.2019.9033053).
- 450 [40] J. I. Novak and J. Loy, "A critical review of initial 3D printed products responding to COVID-19 health
and supply chain challenges," *Emerald Open Research*, vol. 2, p. 24, May 2020, doi: [10.35241/emeraldopenres.13697.1](https://doi.org/10.35241/emeraldopenres.13697.1).
- 451 [41] Y. Y. C. Choong *et al.*, "The global rise of 3D printing during the COVID-19 pandemic," *Nat Rev
452 Mater*, vol. 5, no. 9, pp. 637–639, Sep. 2020, doi: [10.1038/s41578-020-00234-3](https://doi.org/10.1038/s41578-020-00234-3).
- 453 [42] M. Salmi, J. S. Akmal, E. Pei, J. Wolff, A. Jaribion, and S. H. Khajavi, "3D Printing in COVID-
454 19: Productivity Estimation of the Most Promising Open Source Solutions in Emergency Situations,"
Applied Sciences, vol. 10, no. 11, p. 4004, Jan. 2020, doi: [10.3390/app10114004](https://doi.org/10.3390/app10114004).
- 455 [43] M. Attaran, "3D Printing Role in Filling the Critical Gap in the Medical Supply Chain during COVID-
456 19 Pandemic," *American Journal of Industrial and Business Management*, vol. 10, no. 5, pp. 988–1001,
457 May 2020, doi: [10.4236/ajibm.2020.105066](https://doi.org/10.4236/ajibm.2020.105066).

- 451 [44] D. King, A. Babasola, J. Rozario, and J. Pearce, "Mobile Open-Source Solar-Powered 3-D Printers for
452 Distributed Manufacturing in Off-Grid Communities," *Challenges in Sustainability*, vol. 2, Oct. 2014,
doi: [10.12924/cis2014.02010018](https://doi.org/10.12924/cis2014.02010018).
- 453 [45] J. Gwamuri, D. Franco, K. Y. Khan, L. Gauchia, and J. M. Pearce, "High-Efficiency Solar-Powered
454 3-D Printers for Sustainable Development," *Machines*, vol. 4, no. 1, p. 3, Mar. 2016, doi: [10.3390/machines4010003](https://doi.org/10.3390/machines4010003).
- 455 [46] J. Y. Wong, "Ultra-Portable Solar-Powered 3D Printers for Onsite Manufacturing of Medical Re-
456 sources," *Aerospace Medicine and Human Performance*, vol. 86, no. 9, pp. 830–834, Sep. 2015, doi:
[10.3357/AMHP.4308.2015](https://doi.org/10.3357/AMHP.4308.2015).
- 457 [47] M. I. Mohammed, D. Wilson, E. Gomez-Kervin, L. Rosson, and J. Long, "EcoPrinting: Investigation
458 of Solar Powered Plastic Recycling and Additive Manufacturing for Enhanced Waste Management and
Sustainable Manufacturing," in *2018 IEEE Conference on Technologies for Sustainability (SusTech)*,
IEEE, Nov. 2018, pp. 1–6. doi: [10.1109/SusTech.2018.8671370](https://doi.org/10.1109/SusTech.2018.8671370).
- 459 [48] L. Fontana, A. Giubilini, R. Arrigo, G. Malucelli, and P. Minetola, "Characterization of 3D Printed
460 Polylactic Acid by Fused Granular Fabrication through Printing Accuracy, Porosity, Thermal and
Mechanical Analyses," *Polymers*, vol. 14, no. 17, p. 3530, Jan. 2022, doi: [10.3390/polym14173530](https://doi.org/10.3390/polym14173530).
- 461 [49] G. Grassi, S. L. Spagnolo, and I. Paoletti, "Fabrication and durability testing of a 3D printed façade
462 for desert climates," *Additive Manufacturing*, vol. 28, p. 439, 2019.
- 463 [50] A. Petsiuk, B. Lavu, R. Dick, and J. M. Pearce, "Waste Plastic Direct Extrusion Hangprinter," *In-
464 ventions*, vol. 7, no. 3, p. 70, Sep. 2022, doi: [10.3390/inventions7030070](https://doi.org/10.3390/inventions7030070).
- 465 [51] R. S. Rattan, N. Nauta, A. Romani, and J. M. Pearce, "Hangprinter for large scale additive manufac-
466 turing using fused particle fabrication with recycled plastic and continuous feeding," *HardwareX*, vol.
13, p. e00401, Mar. 2023, doi: [10.1016/j.ohx.2023.e00401](https://doi.org/10.1016/j.ohx.2023.e00401).
- 467 [52] A. Alexandre, F. A. Cruz Sanchez, H. Boudaoud, M. Camargo, and J. M. Pearce, "Mechanical Prop-
468 erties of Direct Waste Printing of Polylactic Acid with Universal Pellets Extruder: Comparison to
Fused Filament Fabrication on Open-Source Desktop Three-Dimensional Printers," *3D Printing and
Additive Manufacturing*, vol. 7, no. 5, pp. 237–247, Oct. 2020, doi: [10.1089/3dp.2019.0195](https://doi.org/10.1089/3dp.2019.0195).
- 469 [53] D. J. Byard, A. L. Woern, R. B. Oakley, M. J. Fiedler, S. L. Snabes, and J. M. Pearce, "Green fab
470 lab applications of large-area waste polymer-based additive manufacturing," *Additive Manufacturing*,
vol. 27, pp. 515–525, May 2019, doi: [10.1016/j.addma.2019.03.006](https://doi.org/10.1016/j.addma.2019.03.006).
- 471 [54] M. J. Reich, A. L. Woern, N. G. Tanikella, and J. M. Pearce, "Mechanical Properties and Applications
472 of Recycled Polycarbonate Particle Material Extrusion-Based Additive Manufacturing," *Materials*, vol.
12, no. 10, p. 1642, Jan. 2019, doi: [10.3390/ma12101642](https://doi.org/10.3390/ma12101642).
- 473 [55] H. A. Little, N. G. Tanikella, M. J. Reich, M. J. Fiedler, S. L. Snabes, and J. M. Pearce, "Towards
474 Distributed Recycling with Additive Manufacturing of PET Flake Feedstocks," *Materials*, vol. 13, no.
19, p. 4273, Jan. 2020, doi: [10.3390/ma13194273](https://doi.org/10.3390/ma13194273).
- 475 [56] B. Van de Voorde *et al.*, "Effect of extrusion and fused filament fabrication processing parameters
476 of recycled poly(ethylene terephthalate) on the crystallinity and mechanical properties," *Additive
Manufacturing*, vol. 50, no. 102518, Feb. 2022, doi: [10.1016/j.addma.2021.102518](https://doi.org/10.1016/j.addma.2021.102518).
- 477 [57] S. K. Taghavi, H. Shahrajabian, and H. M. Hosseini, "Detailed comparison of compatibilizers MAPE
and SEBS-g-MA on the mechanical/thermal properties, and morphology in ternary blend of recycled
PET/HDPE/MAPE and recycled PET/HDPE/SEBS-g-MA," *Journal of Elastomers & Plastics*, vol.
50, no. 1, pp. 13–35, 2018.

- 478
- 479 [58] ImageJ, "Image processing and analysis in java." Accessed: Jun. 13, 2023. [Online]. Available:
480 <https://imagej.nih.gov/ij/download.html>
- 481 [59] Y. Pan, G. Wu, H. Ma, S. Zhou, and H. Zhang, "Improved compatibility of PET/HDPE blend by
482 using GMA grafted thermoplastic elastomer," *Polymer-Plastics Technology and Materials*, vol. 59, no.
483 17, pp. 1887–1898, 2020.
- 484 [60] L. Kratofil, Z. Hrnjak-Murgić, J. Jelencć, B. Andrićć, T. Kovacć, and V. Merzel, "Study of the
485 compatibilizer effect on blends prepared from waste poly (ethylene-terephthalate) and high density
486 polyethylene," *International Polymer Processing*, vol. 21, no. 3, pp. 328–335, 2006.
- 487 [61] Jonathan GUIDIGO1 *et al.*, "Polyethylene Low and High Density-Polyethylene Terephthalate and
488 Polypropylene Blend as Matrices for Wood Flour," in *International Journal of Science and Research
(IJSR)*, Jan. 2017, pp. 1069–1074. doi: [10.21275/ART20164296](https://doi.org/10.21275/ART20164296).
- 489 [62] A. Jaisingh Sheoran and H. Kumar, "Fused Deposition modeling process parameters optimization and
490 effect on mechanical properties and part quality: Review and reflection on present research," *Materials
Today: Proceedings*, vol. 21, pp. 1659–1672, Jan. 2020, doi: [10.1016/j.matpr.2019.11.296](https://doi.org/10.1016/j.matpr.2019.11.296).
- 491 [63] S. Oberloier, N. G. Whisman, and J. M. Pearce, "Finding Ideal Parameters for Recycled Materi-
492 al Fused Particle Fabrication-Based 3D Printing Using an Open Source Software Implementa-
493 tion of Particle Swarm Optimization," *3D Printing and Additive Manufacturing*, Apr. 2022, doi:
[10.1089/3dp.2022.0012](https://doi.org/10.1089/3dp.2022.0012).
- 494 [64] S. Oberloier, N. G. Whisman, and J. M. Pearce, "Finding Ideal Parameters for Recycled Materi-
495 al Fused Particle Fabrication-Based 3D Printing Using an Open Source Software Implementa-
496 tion of Particle Swarm Optimization," *3D Printing and Additive Manufacturing*, Apr. 2022, doi:
[10.1089/3dp.2022.0012](https://doi.org/10.1089/3dp.2022.0012).
- 497 [65] Y. Lei, Q. Wu, and Q. Zhang, "Morphology and properties of microfibrillar composites based on recy-
498 cled poly (ethylene terephthalate) and high density polyethylene," *Composites Part A: Applied Science
and Manufacturing*, vol. 40, no. 6, pp. 904–912, Jul. 2009, doi: [10.1016/j.compositesa.2009.04.017](https://doi.org/10.1016/j.compositesa.2009.04.017).
- 499 [66] R. S. Chen, M. H. Ab Ghani, M. N. Salleh, S. Ahmad, and M. A. Tarawneh, "Mechanical, water
500 absorption, and morphology of recycled polymer blend rice husk flour biocomposites," *Journal of
Applied Polymer Science*, vol. 132, no. 8, 2015, doi: [10.1002/app.41494](https://doi.org/10.1002/app.41494).
- 501 [67] M. Bustos Seibert, G. A. Mazzei Capote, M. Gruber, W. Volk, and T. A. Osswald, "Manufacturing
502 of a PET Filament from Recycled Material for Material Extrusion (MEX)," *Recycling*, vol. 7, no. 5,
503 p. 69, Oct. 2022, doi: [10.3390/recycling7050069](https://doi.org/10.3390/recycling7050069).
- 504 [68] M. Nofar and H. Oğuz, "Development of PBT/Recycled-PET Blends and the Influence of Using Chain
Extender," *Journal of Polymers and the Environment*, vol. 27, no. 7, pp. 1404–1417, Jul. 2019, doi:
[10.1007/s10924-019-01435-w](https://doi.org/10.1007/s10924-019-01435-w).
- 505 [69] E. Langer, K. Bortel, S. Waskiewicz, and M. Lenartowicz-Klik, *Methods of PET Recycling*. 2020. doi:
[10.1016/b978-0-323-46200-6.00005-2](https://doi.org/10.1016/b978-0-323-46200-6.00005-2).
- 506 [70] M. S. Saad, A. M. Nor, M. E. Baharudin, M. Z. Zakaria, and A. F. Aimani, "Optimization of sur-
507 face roughness in FDM 3D printer using response surface methodology, particle swarm optimization,
508 and symbiotic organism search algorithms," *The International Journal of Advanced Manufacturing
Technology*, vol. 105, no. 12, pp. 5121–5137, Dec. 2019, doi: [10.1007/s00170-019-04568-3](https://doi.org/10.1007/s00170-019-04568-3).

- 505 [71] A. Selvam, S. Mayilswamy, and R. Whenish, "Strength Improvement of Additive Manufacturing Components by Reinforcing Carbon Fiber and by Employing Bioinspired Interlock Sutures," *Journal of Vinyl and Additive Technology*, vol. 26, no. 4, pp. 511–523, 2020, doi: [10.1002/vnl.21766](https://doi.org/10.1002/vnl.21766).
- 506
- 507 [72] Y. Zhang, S. Wang, and G. Ji, "A Comprehensive Survey on Particle Swarm Optimization Algorithm and Its Applications," *Mathematical Problems in Engineering*, vol. 2015, p. e931256, Oct. 2015, doi: [10.1155/2015/931256](https://doi.org/10.1155/2015/931256).
- 508
- 509 [73] M. Shirmohammadi, S. J. Goushchi, and P. M. Keshtiban, "Optimization of 3D printing process parameters to minimize surface roughness with hybrid artificial neural network model and particle swarm algorithm," *Progress in Additive Manufacturing*, vol. 6, no. 2, pp. 199–215, May 2021, doi: [10.1007/s40964-021-00166-6](https://doi.org/10.1007/s40964-021-00166-6).
- 510
- 511 [74] M. Asadi-Eydivand, M. Solati-Hashjin, A. Fathi, M. Padashi, and N. A. Abu Osman, "Optimal design of a 3D-printed scaffold using intelligent evolutionary algorithms," *Applied Soft Computing*, vol. 39, pp. 36–47, Feb. 2016, doi: [10.1016/j.asoc.2015.11.011](https://doi.org/10.1016/j.asoc.2015.11.011).
- 512
- 513 [75] M. Raju, M. K. Gupta, N. Bhanot, and V. S. Sharma, "A hybrid PSO–BFO evolutionary algorithm for optimization of fused deposition modelling process parameters," *Journal of Intelligent Manufacturing*, vol. 30, no. 7, pp. 2743–2758, Oct. 2019, doi: [10.1007/s10845-018-1420-0](https://doi.org/10.1007/s10845-018-1420-0).
- 514
- 515 [76] J. Cleeman *et al.*, "Scalable, Flexible and Resilient Parallelization of Fused Filament Fabrication:Breaking Endemic Tradeoffs in Material Extrusion Additive Manufacturing," *Additive Manufacturing*, p. 102926, May 2022, doi: [10.1016/J.ADDMA.2022.102926](https://doi.org/10.1016/J.ADDMA.2022.102926).
- 516
- 517 [77] B. Wijnen, P. Sanders, and J. M. Pearce, "Improved model and experimental validation of deformation in fused filament fabrication of polylactic acid," *Progress in Additive Manufacturing*, vol. 3, no. 4, pp. 193–203, Dec. 2018, doi: [10.1007/s40964-018-0052-4](https://doi.org/10.1007/s40964-018-0052-4).
- 518
- 519 [78] J. Shah, B. Snider, T. Clarke, S. Kozutsky, M. Lacki, and A. Hosseini, "Large-scale 3D printers for additive manufacturing: Design considerations and challenges," *The International Journal of Advanced Manufacturing Technology*, vol. 104, no. 9, pp. 3679–3693, Oct. 2019, doi: [10.1007/s00170-019-04074-6](https://doi.org/10.1007/s00170-019-04074-6).
- 520
- 521 [79] A. Roschli *et al.*, "Designing for Big Area Additive Manufacturing," *Additive Manufacturing*, vol. 25, pp. 275–285, Jan. 2019, doi: [10.1016/j.addma.2018.11.006](https://doi.org/10.1016/j.addma.2018.11.006).
- 522
- 523 [80] J. S. Chu, S. C. Koay, M. Y. Chan, H. L. Choo, and T. K. Ong, "Recycled plastic filament made from post-consumer expanded polystyrene and polypropylene for fused filament fabrication," *Polymer Engineering & Science*, vol. 62, no. 11, pp. 3786–3795, 2022, doi: [10.1002/pen.26144](https://doi.org/10.1002/pen.26144).
- 524
- 525 [81] L. J. W. William, S. C. Koay, M. Y. Chan, M. M. Pang, T. K. Ong, and K. Y. Tshai, "Recycling Polymer Blend made from Post-used Styrofoam and Polypropylene for Fuse Deposition Modelling," *Journal of Physics: Conference Series*, vol. 2120, no. 1, p. 012020, Dec. 2021, doi: [10.1088/1742-6596/2120/1/012020](https://doi.org/10.1088/1742-6596/2120/1/012020).
- 526
- 527 [82] N. Verma, P. Awasthi, A. Gupta, and S. S. Banerjee, "Fused Deposition Modeling of Polyolefins: Challenges and Opportunities," *Macromolecular Materials and Engineering*, vol. 308, no. 1, p. 2200421, 2023, doi: [10.1002/mame.202200421](https://doi.org/10.1002/mame.202200421).
- 528
- 529 [83] E. J. Kramer, L. J. Norton, C.-A. Dai, Y. Sha, and C.-Y. Hui, "Strengthening polymer interfaces," *Faraday Discussions*, vol. 98, no. 0, pp. 31–46, Jan. 1994, doi: [10.1039/FD9949800031](https://doi.org/10.1039/FD9949800031).
- 530
- 531 [84] C.-A. Dai *et al.*, "Strengthening Polymer Interfaces with Triblock Copolymers," *Macromolecules*, vol. 30, no. 3, pp. 549–560, Feb. 1997, doi: [10.1021/ma960396s](https://doi.org/10.1021/ma960396s).
- 532

- 533 [85] H. Inoya, Y. Wei Leong, W. Klinklai, S. Thumsorn, Y. Makata, and H. Hamada, "Compatibilization
534 of recycled poly (ethylene terephthalate) and polypropylene blends: Effect of polypropylene molecular
535 weight on homogeneity and compatibility," *Journal of applied polymer science*, vol. 124, no. 5, pp.
536 3947–3955, 2012.
- 535 [86] X. Gao, S. Qi, X. Kuang, Y. Su, J. Li, and D. Wang, "Fused filament fabrication of polymer ma-
536 terials: A review of interlayer bond," *Additive Manufacturing*, vol. 37, p. 101658, Jan. 2021, doi:
537 [10.1016/j.addma.2020.101658](https://doi.org/10.1016/j.addma.2020.101658).
- 537 [87] Y. S. Ko, D. Herrmann, O. Tolar, W. J. Elspass, and C. Brändli, "Improving the filament weld-strength
538 of fused filament fabrication products through improved interdiffusion," *Additive Manufacturing*, vol.
539 29, p. 100815, Oct. 2019, doi: [10.1016/j.addma.2019.100815](https://doi.org/10.1016/j.addma.2019.100815).
- 540 [88] P. Kerdlap, A. R. Purnama, J. S. C. Low, D. Z. L. Tan, C. Y. Barlow, and S. Ramakrishna, "Comparing
541 the environmental performance of distributed versus centralized plastic recycling systems: Applying
542 hybrid simulation modeling to life cycle assessment," *Journal of Industrial Ecology*, vol. 26, no. 1, pp.
543 252–271, 2022, doi: [10.1111/jiec.13151](https://doi.org/10.1111/jiec.13151).
- 544 [89] M. Kreiger and J. M. Pearce, "Environmental Impacts of Distributed Manufacturing from 3-D Printing
545 of Polymer Components and Products," *MRS Proceedings*, vol. 1492, pp. 85–90, Mar. 2013, doi:
546 [10.1557/opl.2013.319](https://doi.org/10.1557/opl.2013.319).
- 547 [90] F. L. Garcia, V. A. da S. Moris, A. O. Nunes, and D. A. L. Silva, "Environmental performance
548 of additive manufacturing process – an overview," *Rapid Prototyping Journal*, vol. 24, no. 7, pp.
549 1166–1177, Jan. 2018, doi: [10.1108/RPJ-05-2017-0108](https://doi.org/10.1108/RPJ-05-2017-0108).
- 550 [91] H. A. Colorado, E. I. G. Velásquez, and S. N. Monteiro, "Sustainability of additive manufacturing:
551 The circular economy of materials and environmental perspectives," *Journal of Materials Research
552 and Technology*, vol. 9, no. 4, pp. 8221–8234, Jul. 2020, doi: [10.1016/j.jmrt.2020.04.062](https://doi.org/10.1016/j.jmrt.2020.04.062).
- 553 [92] K. R. Hart, J. B. Frketic, and J. R. Brown, "Recycling meal-ready-to-eat (MRE) pouches into polymer
554 filament for material extrusion additive manufacturing," *Additive Manufacturing*, vol. 21, pp. 536–543,
May 2018, doi: [10.1016/j.addma.2018.04.011](https://doi.org/10.1016/j.addma.2018.04.011).
- 555 [93] J. Pakkanen, D. Manfredi, P. Minetola, and L. Iuliano, "About the Use of Recycled or Biodegradable
556 Filaments for Sustainability of 3D Printing," in *Sustainable Design and Manufacturing 2017*, G. Cam-
557 pania, R. J. Howlett, R. Setchi, and B. Cimatti, Eds., in Smart Innovation, Systems and Technologies.
Cham: Springer International Publishing, 2017, pp. 776–785. doi: [10.1007/978-3-319-57078-5_73](https://doi.org/10.1007/978-3-319-57078-5_73).
- 558 [94] K. Mikula *et al.*, "3D printing filament as a second life of waste plastics—a review," *Environmental
559 Science and Pollution Research*, vol. 28, no. 10, pp. 12321–12333, Mar. 2021, doi: [10.1007/s11356-020-10657-8](https://doi.org/10.1007/s11356-020-10657-8).
- 560 [95] C. Caceres-Mendoza, P. Santander-Tapia, F. A. Cruz Sanchez, N. Troussier, M. Camargo, and
561 H. Boudaoud, "Life cycle assessment of filament production in distributed plastic recycling
562 via additive manufacturing," *Cleaner Waste Systems*, vol. 5, p. 100100, Aug. 2023, doi:
563 [10.1016/j.clwas.2023.100100](https://doi.org/10.1016/j.clwas.2023.100100).